*Pramana – J. Phys.* (2017) 89:29
DOI 10.1007/s12043-017-1417-9



# Observational constraints on extended Chaplygin gas cosmologies

B C PAUL[1,*], P THAKUR[2] and A SAHA[3]

[1]Physics Department, North Bengal University, Darjeeling 734 013, India
[2]Physics Department, Alipurduar College, Alipurduar 736 122, India
[3]Physics Department, Jalpaiguri Government Engineering College, Jalpaiguri 735 102, India
*Corresponding author. E-mail: bcpaul@iucaa.ernet.in; bcpaul@associates.iucaa.in

MS received 17 June 2016; accepted 25 January 2017; published online 24 July 2017

**Abstract.** We investigate cosmological models with extended Chaplygin gas (ECG) as a candidate for dark energy and determine the equation of state parameters using observed data namely, observed Hubble data, baryon acoustic oscillation data and cosmic microwave background shift data. Cosmological models are investigated considering cosmic fluid which is an extension of Chaplygin gas, however, it reduces to modified Chaplygin gas (MCG) and also to generalized Chaplygin gas (GCG) in special cases. It is found that in the case of MCG and GCG, the best-fit values of all the parameters are positive. The distance modulus agrees quite well with the experimental Union2 data. The speed of sound obtained in the model is small, necessary for structure formation. We also determine the observational constraints on the constants of the ECG equation.

**Keywords.** Modified Chaplygin gas; accelerating Universe; dark energy.

**PACS Nos 04.20.–q; 98.80.Jk; 98.80.–k**

## 1. Introduction

Recent cosmological experiments from a number of observations (e.g., type-Ia supernova [1–4], Wilkinson microwave anisotropy probe (WMAP) [5–9], BAO data [10]) predict that the present Universe is passing through a phase of accelerating expansion. The cause of this acceleration is not understood in the general theory of relativity with ordinary matter fields available from Standard Model of particle physics. It is a present day challenge in theoretical physics to formulate a theory for the observation. The dark energy is considered as a kind of fluid that exerts negative pressure. Several proposals came up in the literature, where either the matter sector or gravitational sector of the Einstein–Hilbert action is discussed. The matter sector is usually considered with exotic matter and one such candidate is Chaplygin gas (CG). The equation of state (henceforth, EoS) for CG is

$$p = -\frac{A}{\rho}, \tag{1}$$

where $A$ is a positive constant. It may be mentioned here that the initial idea of CG originated in aerodynamics [11]. CG may be considered as a viable alternative to quintessence [12]. But CG is ruled out in cosmology as cosmological models are not consistent with observational data namely, SNIa, BAO, CMB and so on [13,14]. Subsequently, the equation of state for CG is generalized to incorporate different aspects of observational Universe. The equation of state for generalized Chaplygin gas (GCG) [15,16] is given by

$$p = -\frac{A}{\rho^{\alpha}}, \tag{2}$$

where $A$ and $0 \leq \alpha \leq 1$ are constants. GCG can explain background dynamics [17] and various other features of a homogeneous isotropic Universe satisfactorily. The matter power spectrum of GCG exhibits strong oscillations or instabilities, unless GCG model reduces to $\Lambda$CDM [18]. Consequently, further modification to GCG has been proposed by adding a positive linear term in density to the EoS, known as modified Chaplygin gas (MCG). The equation of state for MCG is given by

$$p = B\rho - \frac{A}{\rho^{\alpha}}, \tag{3}$$

where $A$, $B$, $\alpha$ are positive constants with $0 \leq \alpha \leq 1$. Thus, MCG is a three-parameter EoS. A cosmological constant $\Lambda$ is emerged by setting $\alpha = -1$ and

$A = 1 + B$. For $A = 0$, eq. (3) reduces to an EoS which describes a perfect fluid with $\omega = B$, e.g., a quintessence model [19]. The MCG model is suitable for obtaining a constant negative pressure at low density accommodating late acceleration and radiation-dominated era (with $B = \frac{1}{3}$) at high density [20]. Wu *et al* [21] studied the dynamics and Bedran *et al* [22] studied the evolution of the temperature function in the presence of MCG. It is also consistent with perturbation study [23]. Cosmological model dominated by viscous dark fluid is also considered in ref. [24]. It is also possible to consider barotropic fluid with quadratic EoS or even with higher-order EoS [25,26]. The extended Chaplygin gas (ECG) is described by

$$p = \sum B_i \rho^i - \frac{A}{\rho^\alpha}, \tag{4}$$

where $A, B_i$ $(i = 1, 2, \ldots)$, $\alpha$ are positive constants with $0 \leq \alpha \leq 1$. In the case of ECG, number of unknowns in the parameter space is increased. We determine here the permitted range of values of the parameters of ECG for viable cosmological scenario employing different observational data in a FRW Universe. We adopt here chi-square minimization technique to obtain constraints imposed by cosmological observations. Defining a total chi-square function, we analyse cosmological models using the $(H(z) - z)$ OHD data (table 1), BAO data (table 2) and CMB data. The constraints on the EoS parameters are determined by drawing contour plots at different confidence levels. The paper is organized as follows: In §2, we set up Einstein field equations and obtain a dimensionless Hubble parameter relevant for the analysis. In §3, we analyse the model with observational data. In §4, the results of the analysis are tabulated. Finally, in §5 we give a general discussion.

## 2. Einstein field equations

The Einstein field equation is given by

$$R_{\mu\nu} - \frac{1}{2} g_{\mu\nu} R = 8\pi G T_{\mu\nu}, \tag{5}$$

where $R_{\mu\nu}$ represents Ricci tensor, $R$ represents Ricci scalar, $T_{\mu\nu}$ represents energy–momentum tensor and $g_{\mu\nu}$ represents the metric tensor in four dimensions. We consider a Robertson–Walker metric which is given by

$$\mathrm{d}s^2 = -\mathrm{d}t^2 + a^2(t) \times \left[ \frac{\mathrm{d}r^2}{1 - kr^2} + r^2(\mathrm{d}\theta^2 + \sin^2\theta\, \mathrm{d}\phi^2) \right], \tag{6}$$

where $k = 0, +1(-1)$ is the curvature parameter in the spatial section representing flat, closed (open) Universe and $a(t)$ is the scale factor of the Universe with $r, \theta, \phi$ being co-moving coordinates.

**Table 1.** Observed Hubble Data with redshift parameter.

| $z$ | $H(z)$ | $\sigma$ | Method | Ref. |
|---|---|---|---|---|
| 0.0708 | 79 | ±19.68 | I | [30] |
| 0.09 | 69.0 | ±12.0 | I | [28] |
| 0.12 | 68.6 | ±26.2 | I | [30] |
| 0.17 | 83.0 | ±8.0 | I | [31] |
| 0.179 | 75.0 | ±4.0 | I | [32] |
| 0.199 | 75.0 | ±5.0 | I | [32] |
| 0.20 | 72.9 | ±29.6 | I | [30] |
| 0.240 | 79.69 | ±2.65 | II | [33] |
| 0.27 | 77.0 | ±14.0 | I | [31] |
| 0.28 | 88.8 | ±36.6 | I | [30] |
| 0.35 | 82.1 | +4.8, −4.9 | I | [34] |
| 0.35 | 84.4 | ±7.0 | II | [35] |
| 0.352 | 83.0 | ±14.0 | I | [32] |
| 0.4 | 95.0 | ±17.0 | I | [31] |
| 0.43 | 86.45 | ±3.68 | II | [33] |
| 0.44 | 82.6 | ±7.80 | II | [36] |
| 0.48 | 97.0 | ±62.0 | I | [37] |
| 0.57 | 92.4 | ±4.5 | II | [38] |
| 0.593 | 104.0 | ±13.0 | I | [32] |
| 0.6 | 87.9 | ±6.1 | II | [36] |
| 0.68 | 92.0 | ±8.0 | I | [32] |
| 0.73 | 97.3 | ±7.0 | II | [36] |
| 0.781 | 105.0 | ±12.0 | I | [32] |
| 0.875 | 125.0 | ±17.0 | I | [32] |
| 0.88 | 90.0 | ±40.0 | I | [37] |
| 0.9 | 117.0 | ±23.0 | I | [31] |
| 1.037 | 154.0 | ±20.0 | I | [32] |
| 1.3 | 168.0 | ±17.0 | I | [31] |
| 1.363 | 160.0 | ±33.6 | I | [39] |
| 1.43 | 177.0 | ±18.0 | I | [31] |
| 1:53 | 140.0 | ±14.0 | I | [31] |
| 1.75 | 202.0 | ±40.0 | I | [31] |
| 1.965 | 186.5 | ±50.4 | I | [39] |
| 2.3 | 224.0 | ±8.0 | II | [40] |
| 2.34 | 222.0 | ±7.0 | II | [41] |
| 2.36 | 226.0 | ±8.0 | II | [42] |

Here the unit of $H(z)$ is km/s/Mpc. I quoted in this table means that the $H(z)$ value is deduced from the differential age method, whereas II corresponds to that obtained from the radial BAO method.

**Table 2.** BAO data.

| $z$ | $\mathcal{A}$ | $\sigma_{\mathcal{A}}$ | Ref. |
|---|---|---|---|
| 0.106 | 0.526 | 0.028 | [46] |
| 0.20 | 0.488 | 0.016 | [46] |
| 0.35 | 0.484 | 0.016 | [46] |
| 0.44 | 0.474 | 0.034 | [43] |
| 0.57 | 0.436 | 0.017 | [44,46] |
| 0.60 | 0.442 | 0.020 | [43] |
| 0.73 | 0.424 | 0.021 | [43] |

**Table 3.** Best-fit values of the EoS parameters for $n = 1$.

| Data | $A_s$ | $B$ | $\alpha$ |
|---|---|---|---|
| OHD + BAO + CMB | 0.9036 | 0.0067 | 0.5218 |

Using metric (6) in the Einstein field eq. (5), we obtain the following equations:

$$3\left(\frac{\dot{a}^2}{a^2}+\frac{k}{a^2}\right)=8\pi G\rho, \tag{7}$$

$$2\frac{\ddot{a}}{a}+\frac{\dot{a}^2}{a^2}+\frac{k}{a^2}=-8\pi Gp, \tag{8}$$

where $\rho$ and $p$ represent the energy density and pressure respectively. The conservation equation is given by

$$\frac{\mathrm{d}\rho}{\mathrm{d}t}+3H(\rho+p)=0, \tag{9}$$

where $H=\dot{a}/a$ is the Hubble parameter.

### 2.1 *For* $n = 1$

For $n = 1$, ECG reduces to EoS corresponding to MCG. Using EoS given by eq. (4) in eq. (9) and then on integrating, one obtains energy density for a MCG which is given by

$$\rho_{\mathrm{ECG11}}=\left[\frac{A}{B+1}+\frac{C}{a^{3(B+1)(\alpha+1)}}\right]^{1/(1+\alpha)}, \tag{10}$$

where $B_1 = B$. The above energy density can be rewritten as

$$\rho_{\mathrm{MCG}}=\rho_0\left[A_s+\frac{1-A_s}{a^{3(1+B)(1+\alpha)}}\right]^{1/(1+\alpha)}, \tag{11}$$

where $A_s = [A/(1+B)][1/\rho_0^{\alpha+1}]$ with $B \neq -1$ and $\rho_0$ is an integration constant. The scale factor of the Universe is related to the redshift parameter $z$ as $(a/a_0) = 1/(1+z)$, where we choose the present scale factor of the Universe $a_0 = 1$ for convenience. The MCG model parameters are $A_s$, $B$ and $\alpha$. From eq. (11), it is evident that the positivity condition of the energy density is ensured when $0 \leq A_s \leq 1$. From eq. (11), one recovers the standard $\Lambda$CDM model for $\alpha = 0$ and $B = 0$. The Hubble parameter can be expressed as a function of redshift using the field eq. (7), which is given by

$$H(z)=H_0[\Omega_{b0}(1+z)^3+(1-\Omega_{b0})[(A_s+(1-A_s)\times(1+z)^{3(1+B)(1+\alpha)})^{1/(1+\alpha)}]]^{1/2}, \tag{12}$$

where $\Omega_{b0}$ and $H_0$ represent the present baryon density and present Hubble parameter respectively. The speed of sound is given by

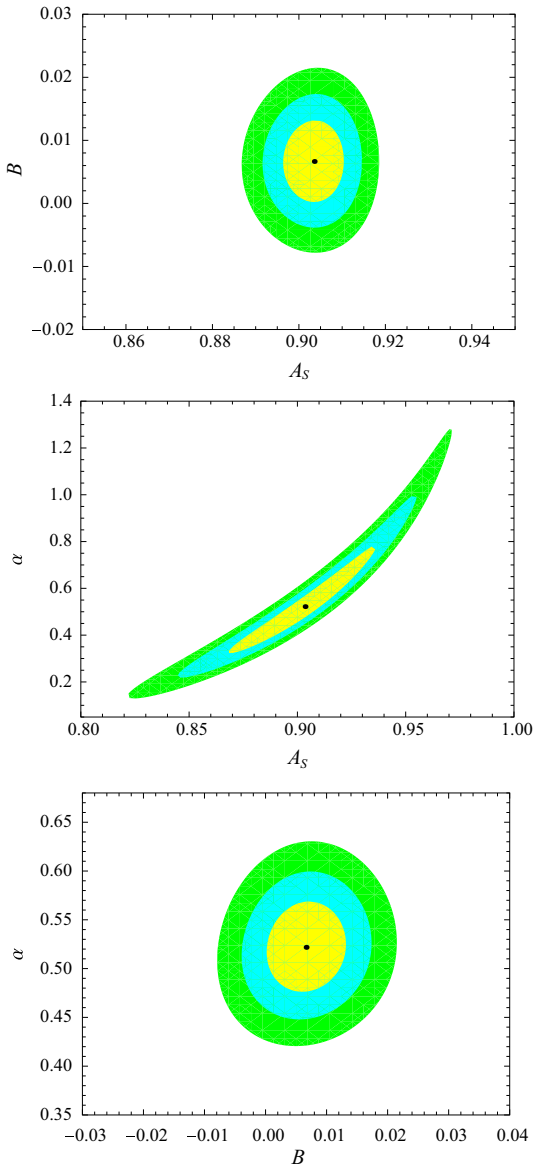


**Figure 1.** Contours from OHD + BAO + CMB at 68.3% (yellow) 95.4% (blue) and 99.7% (green) confidence limit at best-fit values $A_s = 0.9036$, $B = 0.0067$, $\alpha = 0.5218$.

$$c_s^2=\frac{\delta p}{\delta\rho}=\frac{\dot{p}}{\dot{\rho}} \tag{13}$$

which reduces to

$$c_s^2=B+\frac{A_s\alpha(1+B)}{[A_s+(1-A_s)(1+z)^{3(1+B)(1+\alpha)})]}. \tag{14}$$

In terms of EoS it becomes

$$c_s^2=-\alpha\omega+B(1+\alpha). \tag{15}$$

It may be mentioned here that for causality and stability under perturbation it is required to satisfy the inequality condition $c_s^2 \leq 1$ [19].

**Table 4.** Range of values of the EoS parameters $A_s$ and $B$ for $n = 1$.

| Data | CL (%) | $A_s$ | $B$ |
|---|---|---|---|
| OHD + BAO + CMB | 68.3 | (0.896, 0.9101) | (−0.00004, 0.0132) |
| OHD + BAO + CMB | 95.4 | (0.8915, 0.9146) | (−0.0041, 0.0174) |
| OHD + BAO + CMB | 99.7 | (0.8871, 0.9184) | (−0.0077, 0.0215) |

**Table 5.** Range of values of the EoS parameters $A_s$ and $\alpha$ for $n = 1$.

| Data | CL (%) | $A_s$ | $\alpha$ |
|---|---|---|---|
| OHD + BAO + CMB | 68.3 | (0.8684, 0.9354) | (0.3234, 0.7791) |
| OHD + BAO + CMB | 95.4 | (0.8443, 0.9563) | (0.2152, 0.9956) |
| OHD + BAO + CMB | 99.7 | (0.8228, 0.9715) | (0.1297, 1.275) |

**Table 6.** Range of values of the EoS parameters $B$ and $\alpha$ for $n = 1$.

| Data | CL (%) | $B$ | $\alpha$ |
|---|---|---|---|
| OHD + BAO + CMB | 68.3 | (−0.000006, 0.0129) | (0.475, 0.5698) |
| OHD + BAO + CMB | 95.4 | (−0.0041, 0.0175) | (0.4467, 0.6009) |
| OHD + BAO + CMB | 99.7 | (−0.0079, 0.0215) | (0.4212, 0.6292) |

### 2.2 *For* $n = -\alpha$

In this case, the energy density can be expressed as

$$\rho_{\mathrm{ECG21}} = \left[B - A + \frac{C}{a^{3(1+\alpha)}}\right]^{1/(1+\alpha)}, \tag{16}$$

where $B_{-\alpha} = B$. It can also be expressed as

$$\rho_{\mathrm{ECG22}} = \rho_0[A_s + (1 - A_s)(1+z)^{3(1+\alpha)}]^{1/(1+\alpha)}, \tag{17}$$

where

$$A_s = \frac{A - B}{\rho_0^{\alpha+1}}$$

and

$$\rho_0 = (A - B + C)^{1/(1+\alpha)}.$$

Using the field eq. (7), the Hubble parameter can be expressed as a function of redshift which is given by

$$H(z) = H_0[\Omega_{b0}(1+z)^3 + (1 - \Omega_{b0})[A_s + (1 - A_s) \times (1+z)^{3(1+\alpha)}]^{1/(1+\alpha)}]^{1/2}, \tag{18}$$

where $\Omega_{b0}$, $H_0$ represent the present baryon density and present Hubble parameter respectively. The adiabatic squared speed of sound is given by

$$c_s^2 = \frac{\delta p}{\delta \rho} = \frac{\dot{p}}{\dot{\rho}} \tag{19}$$

which reduces to

$$c_s^2 = \frac{A_s \alpha}{[A_s + (1 - A_s)(1+z)^{3(1+\alpha)}]}. \tag{20}$$

In terms of EoS it becomes

$$c_s^2 = -\alpha\omega. \tag{21}$$

In this case also, causality and stability under perturbation is satisfied when $c_s^2 \leq 1$ [19].

### 2.3 *For* $i = n$ *only and* $\alpha = -1$

In this case, the energy density can be expressed as

$$\rho_{\mathrm{ECG31}} = \left[\frac{B}{A-1} + \frac{C}{a^{3(A-1)(n-1)}}\right]^{1/(1-n)}, \tag{22}$$

where $\sum B_n = B$. It can also be expressed as

$$\rho_{\mathrm{ECG32}} = \rho_0[A_s + (1 - A_s)(1+z)^{3(1+\alpha)}]^{1/(1+\alpha)}, \tag{23}$$

where

$$A_s = \frac{B}{A-1}\frac{1}{\rho_0^{1-n}}$$

and

$$C = (1 - A_s)\rho_0^{1-n}.$$

The Hubble parameter in terms of redshift parameter is obtained using field eq. (7), which is given by

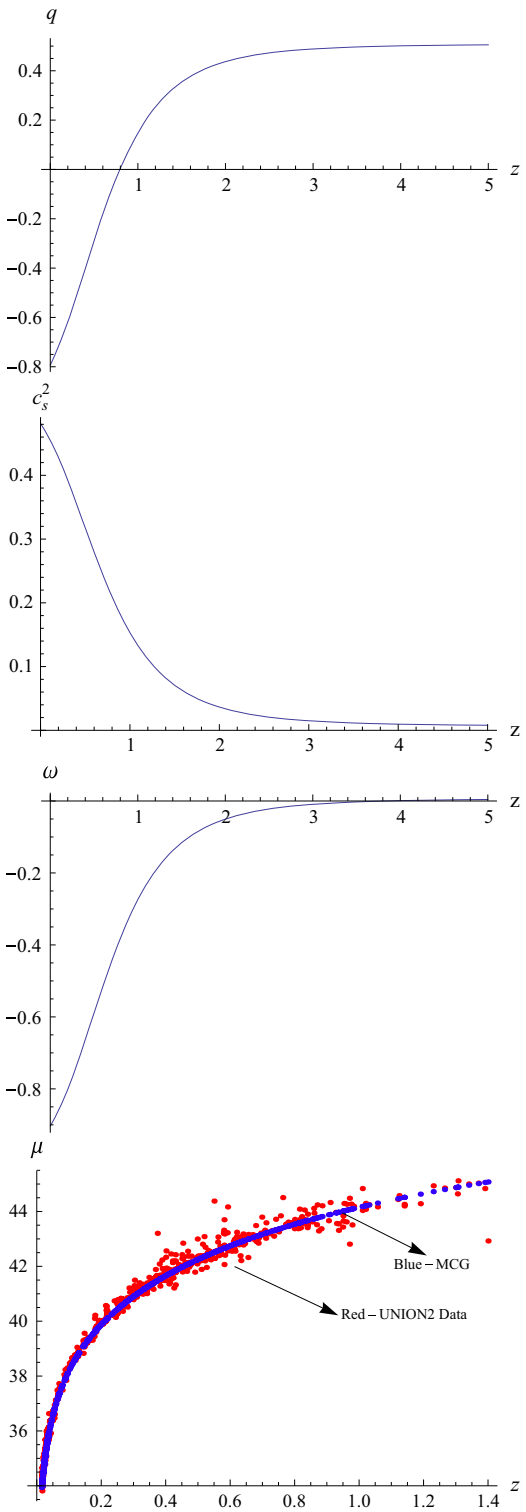


**Figure 2.** Different EoS parameters for MCG in Hubble + BAO + CMB data.

$$H(z) = H_0[\Omega_{b0}(1+z)^3 + (1-\Omega_{b0}) \times [A_s + (1-A_s)(1+z)^{3(A-1)(n-1)}]^{1/(1-n)}]^{1/2} \tag{24}$$

where $\Omega_{b0}$, $H_0$ represent the present baryon density and present Hubble parameter respectively. The adiabatic squared speed of sound is given by

$$c_s^2 = \frac{\delta p}{\delta \rho} = \frac{\dot{p}}{\dot{\rho}} \tag{25}$$

which reduces to

$$c_s^2 = -A + \frac{A_s n(A-1)}{[A_s + (1-A_s)(1+z)^{3(A-1)(n-1)}]}. \tag{26}$$

In terms of EoS it becomes

$$c_s^2 = n\omega + A(n-1). \tag{27}$$

### 2.4 *For* $n = 2$ *and* $\alpha = 1/2$

In this case, EoS given by eq. (4) can be written as

$$p = B_1\rho + B_2\rho^2 - \frac{A}{\rho^{1/2}}. \tag{28}$$

Assuming $B_1 = B_2 = B$ and using eq. (9), the energy density is obtained as

$$\rho = \frac{(Xa^{9/2} + a^{[-(9+15X^2)B]/2})^2}{a^9}, \tag{29}$$

where $X$ is the root of the equation

$$BX^5 + (B+1)X^3 - A = 0. \tag{30}$$

The Hubble parameter is given as

$$H(z) = H_0\left[1 + \frac{(1+z)^{[9(B+1)+15X^2B]/2}}{X^2}\right], \tag{31}$$

where $H_0$ represents the present Hubble parameter.

### 2.5 *For* $n = 3$ *and* $\alpha = 1/2$

In this case, EoS given by eq. (4) becomes

$$p = B_1\rho + B_2\rho^2 + B_3\rho^3 - \frac{A}{\rho^{1/2}}. \tag{32}$$

Assuming $B_1 = B_2 = B_3 = B$ and using eq. (9), the energy density is obtained as

$$\rho = \frac{(Ya^{9/2} + a^{[-(9+15Y^2+21Y^4)B]/2})^2}{a^9}, \tag{33}$$

where $Y$ is the root of the equation

$$BY^7 + BY^5 + (B+1)Y^3 - A = 0. \tag{34}$$

**Table 7.** EoS parameters at different redshift in OHD + BAO + CMB data.

| Data | $z$ | $q$ | $c_s^2$ | $\omega$ |
|---|---|---|---|---|
| OHD + BAO + CMB | 0 | −0.7961 | 0.4793 | −0.9064 |
| Do | $z_t = 0.7801$ | 0 | 0.2031 | −0.3860 |

**Table 8.** Best-fit values of the EoS parameters for $n = -\alpha$.

| Data | $A_s$ | $\alpha$ |
|---|---|---|
| OHD + BAO + CMB | 0.8846 | 0.4056 |

The Hubble parameter is given as

$$H(z) = H_0\left[1 + \frac{(1+z)^{[9(B+1)+15Y^2B+21Y^4B]/2}}{Y^2}\right], \tag{35}$$

where $H_0$ represents the present Hubble parameter.

## 3. Analysis of the cosmological models

### 3.1 *Observed Hubble data*

OHD can be used to constrain cosmological parameters because they are obtained from model-independent direct observations. Until now, two methods have been developed to measure OHD: galaxy differential age and radial BAO size methods. We use thirty Hubble data extracted from the first method and six from the second method as noted in table 1. Jimenez and Loeb [27] first proposed that relative galaxy ages can be used to obtain $H(z)$ values and they reported one $H(z)$ measurement at $z \approx 0.1$ in their later work [28]. Consequently, other Hubble data have been extracted in this method (table 1). In addition, $H(z)$ can also be extracted from the detection of radial BAO features [29]. Gaztanaga *et al* [33] first obtained two $H(z)$ data points using the BAO peak position as a standard ruler in the radial direction. Blake *et al* [36] further combined the measurements of BAO peaks and the Alcock–Paczynski distortion to find three other $H(z)$ results. Samushia *et al* [38] provided a $H(z)$ point at $z = 0.57$ from the BOSS DR9 CMASS sample. To analyse, first we define chi-square ($X^2_{H-z}$) function given by

$$\chi^2_{H-z}(\text{parameters}, z) = \sum \frac{(H(\text{parameters}, z) - H_{\text{obs}}(z))^2}{\sigma_z^2}, \tag{36}$$

where $H_{\text{obs}}(z)$ is the observed Hubble parameter at redshift $z$ and $\sigma_z$ is the error associated with that particular observation are taken from table 1.

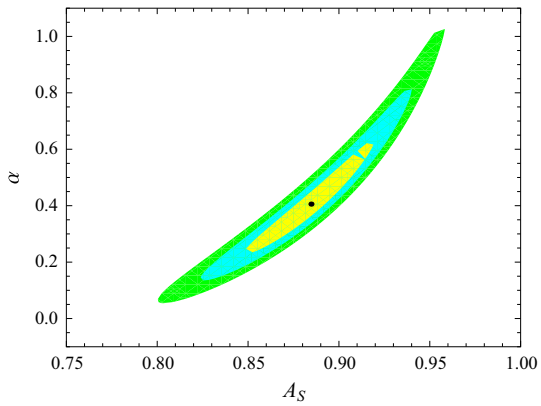


**Figure 3.** Contours from OHD + BAO + CMB data at 68.3% (yellow), 95.4% (blue) and 99.7% (green) confidence limits at best-fit values $A_s = 0.8846, \alpha = 0.4056$.

### 3.2 *BAO peak parameter as a tool for constraining cosmological parameter*

A model-independent BAO (baryon acoustic oscillation) peak parameter can be defined for low redshift ($z_1$) measurements as

**Table 9.** Range of values of the EoS parameters $\alpha$ and $A_s$ for $n = -\alpha$.

| Data | CL (%) | $A_s$ | $\alpha$ |
|---|---|---|---|
| OHD + BAO + CMB | 68.3 | (0.8489, 0.9185) | (0.2296, 0.6246) |
| OHD + BAO + CMB | 95.4 | (0.8236, 0.9415) | (0.1284, 0.8171) |
| OHD + BAO + CMB | 99.7 | (0.7998, 0.9581) | (0.0473, 1.035) |

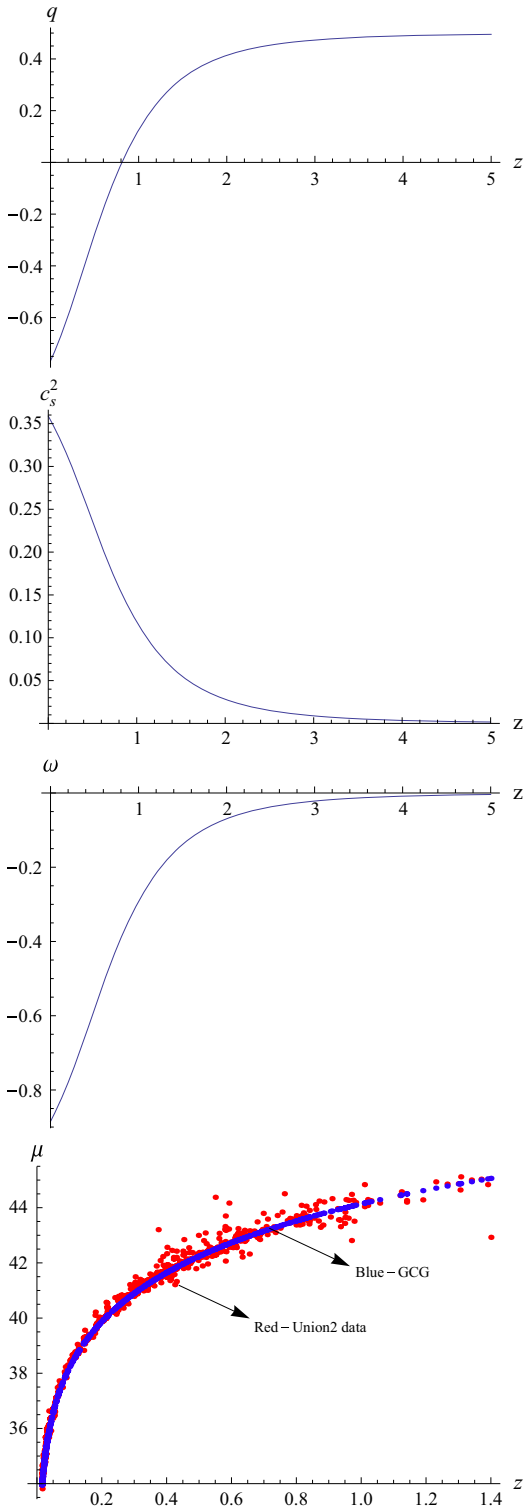


**Figure 4.** Different EoS parameters for GCG in Hubble + BAO + CMB data.

$$\mathcal{A} = \frac{\sqrt{\Omega_m}}{[E(z_1)]^{1/3}} \left[ \frac{\int_0^{z_1} (\mathrm{d}z/E(z))}{z_1} \right]^{2/3}, \tag{37}$$

where $\Omega_m$ is the matter density parameter for the Universe and $E(z) = H(z)/H_0$. For a detailed description of the above defined parameter and related approximations, the reader is referred to [10]. The chi-square function can be defined as

$$\chi^2_{\mathrm{BAO}} = \frac{(\mathcal{A} - \mathcal{A}_{\mathrm{obs}})^2}{(\sigma_{\mathcal{A}})^2}, \tag{38}$$

where we have used the observed data given in table 2.

### 3.3 *CMB shift parameter as a tool for constraining cosmological parameters*

Here the CMB shift parameter is defined as

$$R = \sqrt{\Omega_m} \int_0^{z_{\mathrm{ls}}} \frac{\mathrm{d}z}{E(z)}, \tag{39}$$

where $z_{\mathrm{ls}}$ is the $z$ at the last scattering. The WMAP7 data give us $R = 1.726 \pm 0.018$ at $z_{\mathrm{ls}} = 1091.3$ [45]. Chi-square in this case is defined as

$$\chi^2_{\mathrm{CMB}} = \frac{(R - 1.726)^2}{(0.018)^2}. \tag{40}$$

### 3.4 *Joint analysis with (H−z)+BAO+CMB*

Total chi-square function for the joint analysis is

$$\chi^2_{\mathrm{tot}} = \chi^2_{H-z} + \chi^2_{\mathrm{BAO}} + \chi^2_{\mathrm{CMB}}. \tag{41}$$

The above function will be used in the next section to analyse cosmological models.

## 4. Results of analysis

In this analysis, we consider the baryonic density parameter $\Omega_{bo} = 0.047$ the WMAP [46] and $\Omega_{b0} = 0.0485$ the Planck [47,48] data.

### 4.1 *Case* 1

The best-fit values of the EoS parameters for $n = 1$ are determined from the minimization of chi-squares which are shown in table 3. We obtain best-fit values of EoS parameters which are $A_s = 0.9036$, $B = 0.0067$ and $\alpha = 0.5218$. Using the best-fit values for OHD + BAO + CMB from table 3 we draw contours for the following pairs: (i) $B$ vs. $A_s$ in figure 1a, (ii) $\alpha$ vs. $A_s$ in figure 1b and (iii) $\alpha$ vs. $B$ in figure 1c respectively. Allowed range of values of the EoS parameters are then determined from the contours. In tables 4, 5 and 6, the allowed range of values of $A_s$, $B$ and $\alpha$ for different confidence levels are shown. It is observed that allowed values for $A_s$ and $\alpha$ are always positive but $B$ is

**Table 10.** EoS parameters at different redshift in OHD + BAO + CMB data.

| Data | $z$ | $q$ | $c_s^2$ | $\omega$ |
|---|---|---|---|---|
| OHD + BAO + CMB | 0 | −0.7633 | 0.3608 | −0.884 |
| OHD + BAO + CMB | $z_t = 0.806$ | 0 | 0.1554 | −0.396 |

**Table 11.** Best-fit values of the EoS parameters for $i = n$ and $\alpha = 1$.

| Data | $A_s$ | $A$ | $n$ |
|---|---|---|---|
| OHD + BAO + CMB | 0.9028 | −0.0066 | −0.5146 |

found with both positive and negative values. The permitted range of values of $A_s$ and $B$ lies in the range (0.8871, 0.9184) and (−0.0077, 0.0215); $A_s$ and $\alpha$ lie in the range (0.8228, 0.9715) and (0.1297, 1.275); $B$ and $\alpha$ lie in the range (−0.0079, 0.0215) and (0.4212, 0.6292) at 99.7% confidence level.

In this case, the deceleration parameter ($q$), the adiabatic squared speed of sound ($c_s^2$), the EoS parameter ($\omega$) and distance modulus ($\mu$) are plotted with redshift parameter in figure 2. The deceleration parameter, squared speed of sound and the EoS parameter at the present epoch attains −0.7961, 0.4793 and −0.9064 respectively (shown in table 7). The magnitude of transition redshift is $z_t = 0.7801$ when the Universe entered into the present accelerating phase (tables 8, 9).

### 4.2 *Case* 2

In this case, the best-fit values of $A_s$ and $\alpha$ are 0.8846 and 0.4056 respectively for the cosmological model with $n = -\alpha$. Using these values, we analyse and found the range of values of $A_s$, $\alpha$ as (0.7998, 0.9581) and (0.0473, 1.035) respectively at 99.7% confidence level are shown in figure 3. In this case, the deceleration parameter ($q$), the adiabatic squared speed of sound ($c_s^2$), the EoS parameter ($\omega$) and distance modulus ($\mu$) are plotted with redshift parameter in figure 4. The deceleration parameter, squared speed of sound and the EoS parameter at the present epoch attains −0.7633, 0.3608 and −0.8844 respectively (shown in table 10). The magnitude of transition redshift is $z_t = 0.806$ when the Universe entered into the present accelerating phase.

### 4.3 *Case* 3

In this case, the best-fit values of $A_s$, $A$ and $n$ are given in table 11 for $i = 1$ and $\alpha = -1$.

The best-fit values of $A_s$, $A$ and $n$ are 0.9028, −0.0066 and −0.5146 respectively. In figure 5 contours are drawn for $n-A$, $A-A_s$ and $n-A$ respectively to obtain the constraints imposed on them from observations.

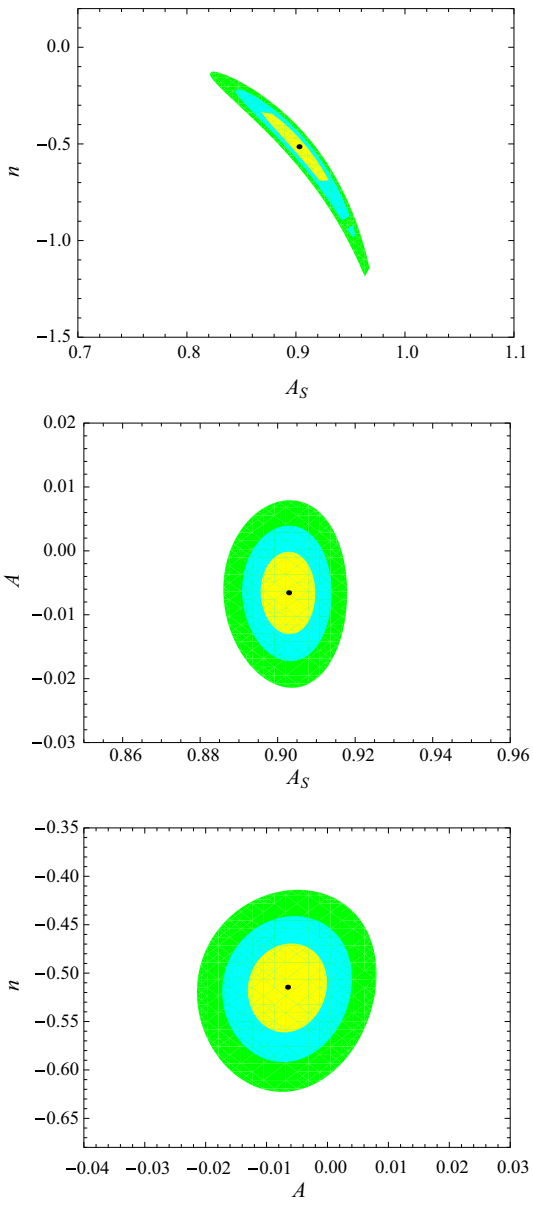


**Figure 5.** Contours from OHD + BAO + CMB data at 68.3% (yellow), 95.4% (blue) and 99.7% (green) (dotted) confidence limits at best-fit values $A_s = 0.9028$, $A = -0.0066$, $\alpha = -0.5146$.

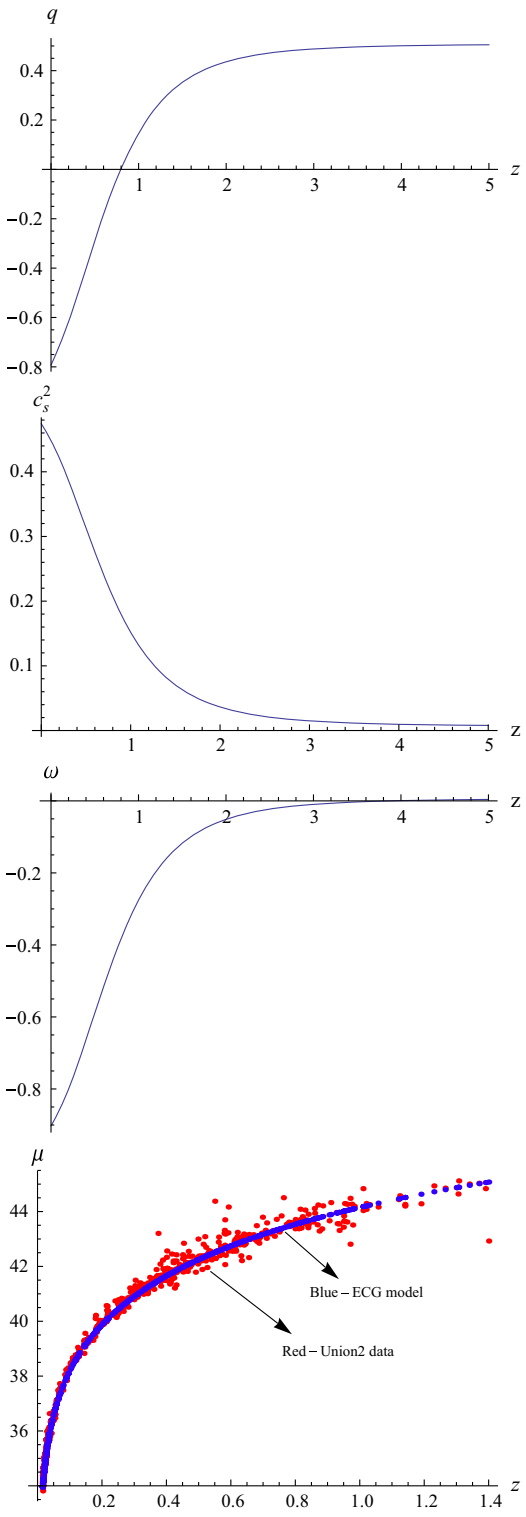


**Figure 6.** Different EoS parameters for ECG in Hubble + BAO + CMB data.

In this case, the deceleration parameter ($q$), the adiabatic squared speed of sound ($c_s^2$), the EoS parameter ($\omega$) and distance modulus ($\mu$) are plotted with redshift parameter in figure 6. The deceleration parameter, squared speed of sound and the EoS parameter at the present epoch attains $-0.7961$, $0.4793$ and $-0.9064$ respectively. The magnitude of transition redshift is $z_t = 0.7801$ when the Universe entered into the present accelerating phase.

### 4.4 *Case* 4

In this case, we find that the best-fit values of $X$ and $B$ for $n = 2$ and $\alpha = \frac{1}{2}$ are 2.83633 and $-0.037662$ respectively.

### 4.5 *Case* 5

In this case, the best-fit values of $Y$ and $B$ are 2.83641 and $-0.00328$ respectively for $n = 3$ and $\alpha = \frac{1}{2}$.

## 5. Discussion

We present cosmological models with ECG as a candidate for dark energy and determine the allowed range of values of the EoS parameters by using the observed data. In the numerical analysis we consider two fluids, namely, (i) modified Chaplygin gas (MCG), (ii) generalized Chaplygin gas (GCG), as special cases of a more general EoS termed as extended Chaplygin gas (ECG). In the case of MCG, the best-fit values of all the parameters are found to be positive definite. But $B$ is found to take both positive as well as negative values while $A_s$ and $\alpha$ are positive within 99.7% confidence level. The distance modulus obtained from the best-fit parameters of this model agrees quite well with the observed Union2 data [52] as shown in figure 2. The squared speed of sound obtained in the model is small which permits structure formation. Thus, the MCG model is a good candidate for describing evolution of the Universe which reproduces cosmic growth with inhomogeneity in addition to a late-time accelerating phase.

In the case of GCG, the best-fit values of $A_s$ and $\alpha$ are found to be positive within 99.7% confidence level and they remain positive. The distance modulus agrees quite well with the experimental Union2 data [52] as shown in figure 4. The speed of sound obtained in the model is also small. Thus, the GCG model reproduces cosmic growth with inhomogeneity in addition to a late-time accelerating phase as shown by the plot of $q$ and $\omega$. When $n = 2$ and $\alpha = 1/2$, the best-fit values for $X$ and $B$ are 2.83633 and $-0.037662$ respectively. When $n = 3$ and $\alpha = 1/2$, the best-fit values of $Y$ and $B$ are 2.83641 and $-0.00328$ respectively. In table 10, it is evident that $\omega < -1/3$ attains a small negative value at the present epoch. In table 12, it is evident that in the case of MCG $\alpha$ is bigger than GCG, but $B$ picks up a small positive value.

**Table 12.** Comparison of the values of EoS parameters for GCG and MCG models.

| Model | Data | $A_s$ | $\alpha$ | $B$ | Ref. |
|---|---|---|---|---|---|
| GCG | Supernovae | 0.6–0.85 | – | 0.0 | [49] |
| GCG | CMBR | 0.81–0.85 | 0.2–0.6 | 0.0 | [50] |
| GCG | WMAP | 0.78–0.87 | – | 0.0 | [14] |
| GCG | CMBR + BAO | $\approx 0.77$ | $\leq 0.1$ | 0.0 | [51] |
| GCG | OHD + BAO + CMB | 0.8846 | 0.4056 | 0.0 | This paper |
| MCG | OHD + BAO + CMB | 0.9036 | 0.5218 | 0.0067 | This paper |

The suitability of the cosmological model in the presence of ECG is also studied by plotting the distance modulus $\mu$ with variation of redshift in figure 6 which is then compared with Union2 data also.

## Acknowledgements

BCP would like to thank IUCAA Reference Centre at North Bengal University. PT would like to thank IUCAA Reference Centre at North Bengal University for extending necessary research facilities to initiate the work.

## References

[1] S Perlmutter *et al*, *Nature* **391**, 51 (1998)
[2] S Perlmutter *et al*, *Astrophys. J.* **517**, 565 (1999)
[3] A G Riess *et al*, *Astron. J.* **116**, 1009 (1998)
[4] J L Tonry *et al*, *Astrophys. J.* **594**, 1 (2003)
[5] S Bridle, O Lahav, J P Ostriker and P J Steinhardt, *Science* **299**, 1532 (2003)
[6] C L Bennett *et al*, *Astrophys. J. Suppl.* **148**, 1 (2003)
[7] G Hinshaw *et al*, *Astrophys. J. Suppl.* **148**, 135 (2003)
[8] A Kogut *et al*, *Astrophys. J. Suppl.* **148**, 161 (2003)
[9] D N Spergel *et al*, *Astrophys. J. Suppl.* **148**, 175 (2003)
[10] D J Eisenstein *et al*, *Astrophys. J.* **633**, 560 (2005)
[11] S Chaplygin, *Sci. Mem. Moscow Univ. Math. Phys.* **21**, 1 (1904)
[12] A Kamenshchik, U Moschella and V Pasquier, *Phys. Lett. B* **511**, 265 (2001)
[13] Z H Zhu, *Astron. Astrophys.* **423**, 421 (2004)
[14] M C Bento, O Bertolami and A A Sen, *Phys. Lett. B* **575**, 172 (2003)
[15] N Bilic, G B Tupper and R D Viollier, *Phys. Lett. B* **535**, 17 (2001)
[16] M C Bento, O Bertolami and A A Sen, *Phys. Rev. D* **66**, 043507 (2002)
[17] J C Fabris, P L C de Oliveira and H E S Velten, *Eur. Phys. J. C* **71**, 1773 (2011)
[18] H Sandvik, M Tegmark, M Zaldarriaga and I Waga, *Phys. Rev. D* **69**, 123524 (2004)
[19] Lixin Xu, Yuting Wang and Hyerim Noh, *Eur. Phys. J. C* **72**, 1931 (2012)
[20] U Debnath, A Banerjee and S Chakraborty, *Class. Quant. Grav.* **21**, 5609 (2004)
[21] Y Wu, S Li, J Lu and X Yang, *Mod. Phys. Lett. A* **22**, 783 (2007)
[22] M L Bedran, V Soares and M E Araujo, *Phys. Lett. B* **659**, 462 (2008)
[23] S Costa, M Ujevic and A F dos Santos, *Gen Relativ. Gravit.* **40**, 1683 (2008)
[24] H Velten and B J Schwarz, *J. Cosmol. Astropart. Phys.***09**, 016 (2011)
[25] E V Linder and R J Scherrer, *Phys. Rev. D* **80**, 023008 (2009)
[26] F Rahman, M Jamil and K Chakraborty, *Astrophys. Space Sci.* **331**, 191 (2011)
[27] R Jimenez and A Loeb, *Astrophys. J.* **573**, 37 (2002)
[28] R Jimenez *et al*, *Astrophys. J.* **593**, 622 (2003)
[29] T-J Zhang, C Ma and T Lan, *Adv. Astron.* **2010**, 81 (2010)
[30] C Zhang *et al*, *Res. Astron. Astrophys.* **14**, 1221 (2014)
[31] J Simon *et al*, *Phys. Rev. D* **71**, 123001 (2005)
[32] M Moresco *et al*, *J. Cosmol. Astropart. Phys.* **8**, 6 (2012)
[33] E Gaztanaga *et al*, *Mon. Not. R. Astron. Soc.* **399**, 1663 (2009)
[34] C-H Chuang *et al*, *Mon. Not. R. Astron. Soc.* **426**, 226 (2012)
[35] X Xu *et al*, *Mon. Not. R. Astron. Soc.* **431**, 2834 (2013)
[36] C Blake *et al*, *Mon. Not. R. Astron. Soc.* **425**, 405 (2012)
[37] D Stern *et al*, *J. Cosmol. Astropart. Phys.* **1002**, 008 (2010)
[38] L Samushia *et al*, *Phys. Rev. D* **86**, 103527 (2012)
[39] M Moresco, *Mon. Not. R. Astron. Soc.* **450**, L16 (2015)
[40] N G Busca *et al*, *Astron. Astrophys.* **552**, A96 (2013)
[41] T Delubac *et al*, *Astron. Astron.* **574**, A59 (2015)
[42] A Font-Ribera *et al*, *J. Cosmol. Astropart. Phys.* **5**, 27 (2014)
[43] C Blake *et al*, *Mon. Not. R. Astron. Soc.* **418(3)**, 1707 (2011)
[44] C-H Chuang *et al*, *Mon. Not. R. Astron. Soc.* **433(4)**, 3559 (2013)
[45] E Komatsu *et al*, 2010, arXiv:1001.4538 [astro-ph.CO]
[46] WMAP Collaboration: G Hinshaw *et al*, *Astrophys. J. Suppl.* **208**, 19 (2013)
[47] Planck Collaboration: P A R Ade *et al*, *Astron. Astrophys.* **571**, A16 (2014)
[48] Planck Collaboration: P A R Ade *et al*, arXiv:1502.01589 [astro-ph.CO].

[49] M Makler, S D de Oliveira and I Waga, *Phys. Lett. B* **555**, 1 (2003)
[50] M C Bento, O Bertolami and A A Sen, *Phys. Rev. D* **67**, 063003 (2003)
[51] T Barriero, O Bertolami and P Torres, *Phys. Rev. D* **78**, 043530 (2008)
[52] S Wang, X-D Li and M Li, *Phys. Rev. D* **83**, 023010 (2011)